TNO innovation for life

A tool to assess the capacity for storage of carbon dioxide in deep saline aquifers

SCADSA - Storage Capacity Assessment for Deep Saline Aquifers

TNO Public › R2025 R10218
20 February 2025

Energy & Materials Transition
www.tno.nl
+31 88 866 42 56
info@tno.nl

R2025 R10218 – 20 February 2025

SCADSA - Storage Capacity Assessment for Deep Saline Aquifers

A tool to assess the capacity for storage of carbon dioxide in deep saline aquifers

Author(s)	T. (Thomas) Ravestein, B. (Bart) Davids, J.M. (Jo) van Buggenum

Classification report	TNO Public
Number of copies	TNO Public
Report text	TNO Public
Number of pages	16 (excl. front and back cover)
Number of appendices	0
Sponsor	Ministry of Economic Affairs and Climate Policy
Programme name	EZK Work Program 2024
Programme number	060.58401
Project name	CO2 Capacity Prognosis
Project number	01.06.03

Summary

This document describes the method developed for the SCADSA tool, SCADSA stands for Storage Capacity Assessment for Deep Saline Aquifers. This tool was developed by TNO-AGE in 2023-2024 to assess the theoretical capacity for storage of carbon dioxide (CO_2) in deep saline sandstone aquifer complexes. It can calculate the storage capacity per aquifer complex based on an analytical model using a deterministic and probabilistic approach. It utilizes the Microsoft Excel platform, see the User Guide (Van Buggenum et al., 2024b) for more guidance on its usage.

Contents

1 Introduction

1.1 Definitions & nomenclature

SCADSA stands for the tool Storage Capacity Assessment for Deep Saline Aquifers. It is a tool that allows the user to asses the storage capacity of carbon dioxide (CO_2) in confined aquifers. It has an accompanying document, the SCADSA user guide (Van Buggenum 2024b), in which the tool layout is described and practical guidelines how choose parameters are discussed. This report discusses the methodology of the tool discussed.

CO_2 storage is theoretically possible in closed system (Gammer et al., 2011) deep saline aquifers. In such a system the aquifer is not or in limited contact with the sea and therefore unable to balance its pressures with the surroundings during operational timescales.

When CO_2 is injected into a closed aquifer system, storage space is created by compressing the water and deforming the formation rock. The reservoir pore fluid pressure will increase accordingly (see Figure 1). The storage capacity is then bounded by, amongst others, a maximum pressure at the crest of the aquifer, beyond which the sealing integrity of the cap rock could be lost and leakage of CO_2 potentially occurs. Other effects can cause leakage of CO_2 from the aquifer (e.g. injection induced fault reactivation and subsequent leakage) and have not been taken into account, because these causes are outside of the scope of this project.

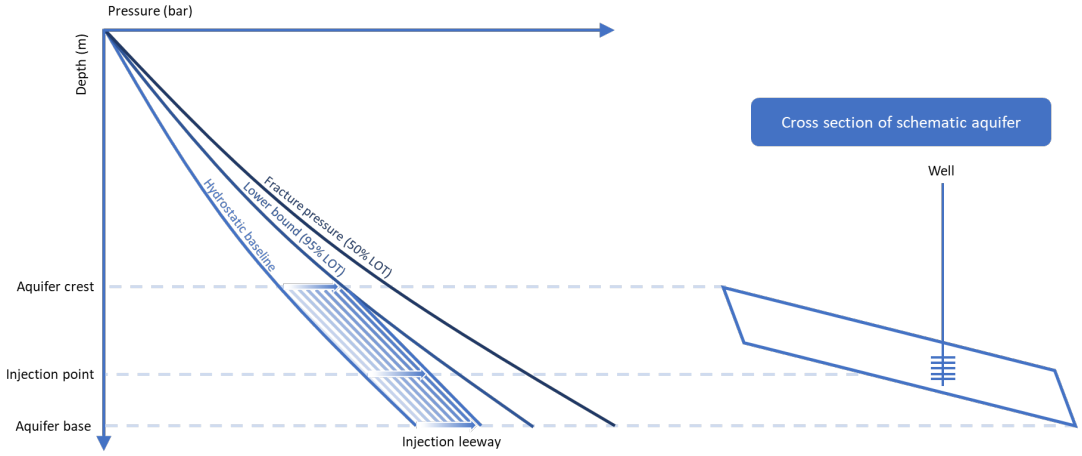

Figure 1: A schematic overview of the pressure gradients by which the maximum increase in pressure is limited.

1.2 Background

The SCADSA tool was developed by TNO-AGE in 2023-2024 to assess the theoretical capacity for storage of carbon dioxide (CO_2) in deep saline sandstone aquifer complexes. It allows the user to calculate the storage capacity per aquifer complex with a deterministic and probabilistic approach. It utilizes the Microsoft Excel platform, see the User Guide (Van Buggenum et al., 2024b) for more guidance on its usage.

The theoretical storage capacity is calculated using an analytical model described here. The theoretical storage capacity is the maximum amount of CO_2 that can be stored in the aquifer under ideal static conditions, which means it assumes only the maximum structural trapping of injected CO_2. Dynamic processes such as injectivity and time for pressure and fluid to balance within the aquifer are not considered. Therefore, the tool cannot assess the storage capacity of unconfined saline aquifers in which pressure can escape the complex, nor can it calculate the storage capacity associated with CO_2 solution and mineral trapping.

The theoretical storage capacity is determined by the volume of the formation available to CO_2 storage, the density of the CO_2 and an efficiency factor (Bentham et al., 2014). The latter comprises the allowed pore pressure increase of the aquifer (bar) and the total compressibility of fluid and rock (1/bar).

The theoretical storage capacity is considered a first-order estimate of storage potential for CO_2 in deep saline aquifers with a large uncertainty. This can subsequently be narrowed down by estimating the effective or practical storage capacity due to geological, technical, economic, and legislative constraints (see Figure 2).

To capture the range of the aforementioned uncertainty, the SCADSA tool can be used probabilistically and deterministically, as explained in the following chapter.

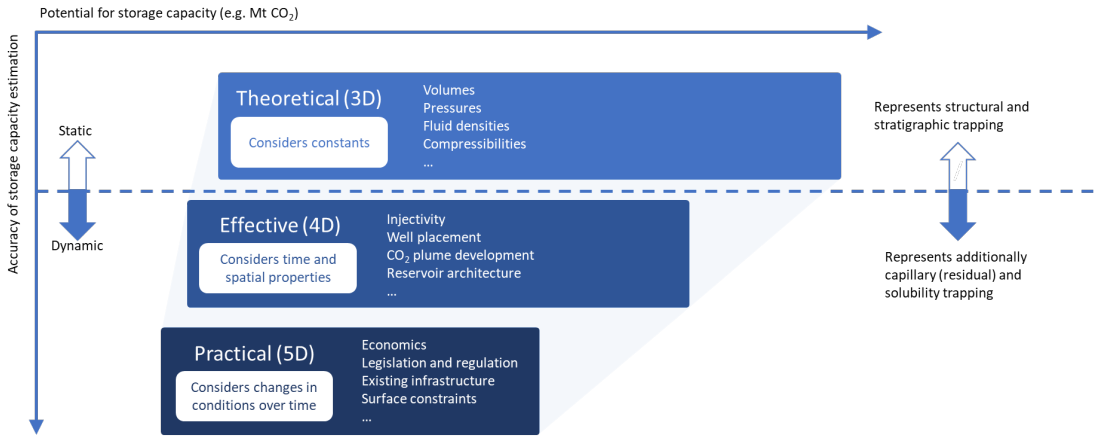

Figure 2: From theoretical to effective to practical storage capacity, the accuracy of the capacity estimation increases while the range in potential decreases. Note that the step from theoretical to effective and practical requires dynamic reservoir simulation, which is out of scope for this tooling.

2 Methods

The methods used for the tool are consecutively described for the deterministic and probabilistic approach. Both are displayed on the “Probabilistic Capacity” tab of the tool.

2.1 Deterministic capacity assessment

The deterministic approach uses 15 input parameters, that after several intermediate computations, result in values for four elements required for the capacity assessment and the CO_2 mass calculation:

1. Formation pore volume (V_{pore});
2. Allowed pressure increase (ΔP_{crest});
3. Total compressibility, and (C_{total});
4. CO_2 density (ρ_{CO_2}).

The assumptions for each input parameter and the intermediate computations are given below. For the application of each input parameter, see the user guide (Van Buggenum et al., 2024b).

The 15 input parameters including their notation, name in the SCADSA tool and user guide and unit:

- z_c Aquifer crest (mTVDss)
- z_b Aquifer base (mTVDss)
- $\frac{dP_w}{dz}$ Hydrostatic gradient (bar/10m)
- $P_{crest}^{initial}$ Initial pressure at crest (bar)
- $P_{crest}^{allowed}$ Maximum allowed pressure at crest (bar)
- h_{CO_2} Plume height (m)
- $\frac{dT}{dz}$ Temperature gradient (°C/km)
- S Brine salinity (ppm)
- C_{solid} Solid rock compressibility (1/bar)
- C_{frame} Frame compressibility (1/bar)
- A Area of aquifer (m^2)
- H Thickness of aquifer (m)
- NtG Net-to-Gross ratio (-)
- ϕ Porosity (-)
- V_{bulk} Bulk volume of aquifer (m^3)

The entered parameters are applied as constants throughout the aquifer. It is recommended to use the average values of the aquifer for most representative results.

Formation pore volume

The formation pore volume (V_{pore}) calculation assumes a rectangular, isotropic, homogeneous box that neglects any dip angle: $V_{pore} = A\ H\ NtG\ \phi$, with the option to insert $V_{bulk} = A\ H$ directly, using a predetermined value from e.g. a 3D static geological model or maps.

Aquifer storage pressures

In Figure 3 a simplified representation of the pressure-depth profile shown in the SCADSA tool is given. The parameters C to H are determined in the SCADSA tool, as is the hydrostatic and lithostatic baseline and the mid LB-FG profile (dark blue, solid gray and red line in Figure 3). For definition and derivation of these profiles see Van Buggenum (2024a).

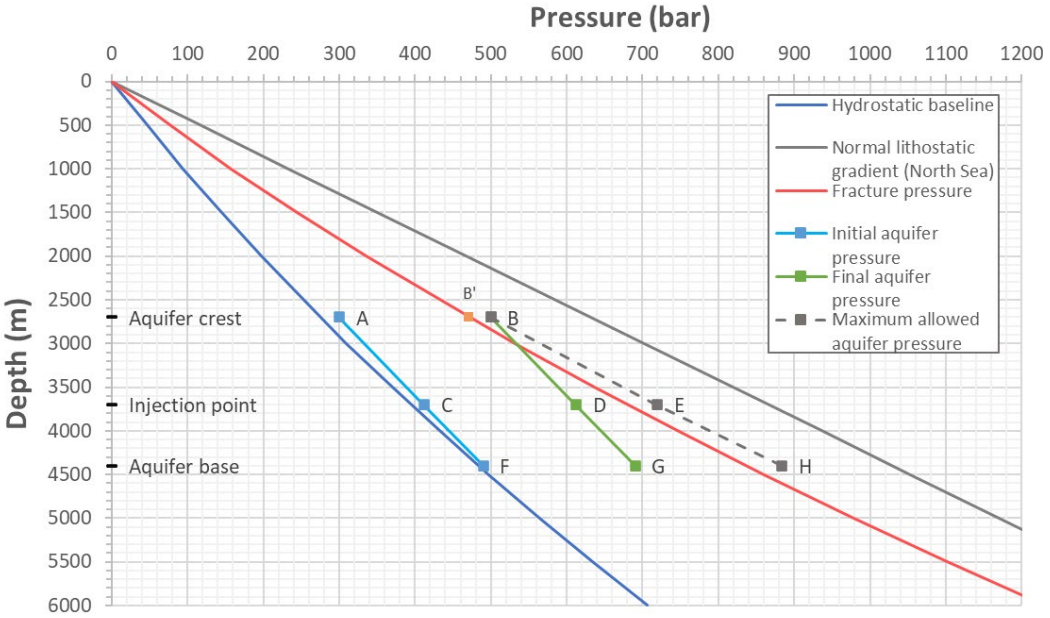

Figure 3: Aquifer storage complex pressures. This figure illustrates the pressure profiles of a generic aquifer complex, with the crest located at 2700 m and the base at 4400 m. The profiles depicting pressure over the aquifer depth are shown both before CO_2 injection (line A-F) and after CO_2 injection (line B-G). The maximum allowable pressures at each depth in the aquifer are denoted by line B-H, where the injection leeway is defined as the interval between point D and point E. In addition, the hydrostatic baseline, lithostatic pressure and fracture pressure are shown. It should be noted that a reasonable assumption is that the maximum allowed pressure is below the fracture pressure profile.

In Figure 3, A and B are the input parameters $P_{crest}^{initial}$ and $P_{crest}^{allowed}$. The lithostatic gradient (grey line) assumes a density of 2340 kg/m^3, which once converted to bar, gives a profile that follows the linear function $0.234z$, assuming a gravitational acceleration of 10 m/s^2. Please note that this lithostatic gradient is purely for visualization purposes.

The hydrostatic profile (dark blue line in Figure 3) is defined as:

Equation 1: Empirical relationship between hydrostatic pressure ($P_{hydrostatic}$) and depth (z) for the Dutch offshore.

$$P_{hydrostatic}(z) = 4.9 \times 10^{-6} z^2 + 0.088z + 1.81$$

The hydrostatic baseline as expressed above is derived in Van Buggenum et al., 2024a. The fracture pressure profile is the upper bound of the mud weight used during drilling operations and is defined as follows (Van Buggenum et al., 2024a):

Equation 2: Empirical relationship between fracture pressure and depth for the Dutch offshore.

$$P_z^{frac}(z) = 9.2e^{-6}z^2 + 0.15z - 1$$

of which B' in Figure 3 is the fracture pressure profile evaluated at the aquifer crest (where $z = z_c$).

The points C and F are $P_{injection}^{initial}$ and $P_{base}^{initial}$ and are dependent on the hydrostatic gradient $\frac{dP_w}{dz}$ by evaluating Equation 3 at $z = z_{injection}$ and $z = z_{base}$ respectively.

Equation 3: Relationship between pressure through depth inside an aquifer with known $P_{crest}^{initial}$.

$$P_z^{initial}\left(z, \frac{dP_w}{dz}, z_c\right) = P_{crest}^{initial} + \frac{\frac{dP_w}{dz}(z - z_c)}{10}$$

The allowed pressure increase of the entire aquifer is focused on the pressure increase at the crest of the aquifer (Δp_{crest}), because it is assumed that at that point a pressure limit will be reached the earliest across the depth of the entire aquifer (recall Figure 3). In case another depth is a limiting factor (e.g. because another potential leak path with a lower pressure threshold is at that depth) this depth is replaced with the depth of the crest. The allowed pressure increase is calculated by computing the difference between the initial and allowed pressure at the crest of the aquifer:

Equation 4: The ΔP is the difference between the allowed and initial pressure at the crest.

$$\Delta P_{crest} = P_{crest}^{allowed} - P_{crest}^{initial}$$

The points D and G from Figure 3 are determined by adding ΔP_{crest} to C and F.

Any overpressure that might be present before injection is calculated by taking the difference between the hydrostatic baseline at z_c and $P_{crest}^{initial}$.

Since B can be defined by the user independently from the default pressure profile, the behavior of E and H over depth are interpolated to always fall with constant proportionality between the LOT (Leak Off Test) lower boundary and fracture pressure gradients. The LOT lower boundary is defined as (Van Buggenum et al., 2024a):

Equation 5: Relationship between LOT lower boundary and depth.

$$P_z^{LOT\ lower\ boundary}(z) = 1.0 \times 10^{-5}z^2 + 0.115z + 5$$

The interpolation factor (f_i) is then defined as:

Equation 6: Definition of the interpolation factor.

$$f_i = \frac{P_{crest}^{allowed} - P_{crest}^{LOT\ lower\ boundary}}{P_{crest}^{frac} - P_{crest}^{LOT\ lower\ boundary}}$$

The relationship of $P_{allowed}$ over depth is defined as:

Equation 7: Relationship between allowed pressure and depth.

$$P_z^{allowed}(z) = P_z^{LOT\ lower\ boundary}(z) + f_i\left(P_z^{frac}(z) - P_z^{LOT\ lower\ boundary}(z)\right)$$

The pressures E and F ($P_{injection}^{allowed}$ and $P_{base}^{allowed}$ respectively) are determined by evaluating Equation 7 at depths $z = z_{injection}$ and $z = z_b$.

Total compressibility

Total compressibility (C_{total}) is the compressibility of both the brine (C_{brine}) and the pore space (C_{pore}): $C_{total} = C_{brine} + C_{pore}$.

The brine compressibility C_{brine} is based on Whitson & Brulé (2000), which depends on the formation pressure, temperature and salinity, and can be calculated based on the following empirical relationships:

Equation 8: Relationship between brine compressibility and pressure and temperature.

$$C_{brine} = (A_1 + A_2 P)^{-1}$$

Where:
$A_1 = 10^6(0.314 + 0.58w_s + 1.9 \times 10^{-4}T - 1.45 \times 10^{-6}T^2)$
$A_2 = 8 + 50w_s - 0.125w_sT$

Where pressure P is in psi, water salinity w_s is in weight fraction (e.g. 0.2 w_s equals 200.000 ppm) and temperature T is in °F. In order to be able to use the Whitson & Brule (2000) relationships, the tool converts the 1/psi output into 1/bar by dividing it by 0.0689 and converts °C to °F using $1.8\,°C + 32$.

The pore space compressibility C_{pore} is based on Fjaer (2021, formula 1.205):

Equation 9: Relationship between pore compressibility, porosity and the compressibility of the rock frame and grains.

$$C_{pore}(C_{frame}, C_{solid}, \phi) = \frac{C_{frame} - \left(C_{solid}(1+\phi)\right)}{\phi}$$

where C_{frame} is the compaction coefficient of the rock's frame: the supporting structure of stacked grains. It is by default assumed to be dependent on only porosity according to a regression done by TNO (2013) on porosity measurements on Dutch Rotliegend sandstones:

Equation 10: Relationship between frame compressibility and porosity for Dutch Rotliegend sandstone.

$$C_{frame}(\phi) = 4.943 \times 10^{-3}\phi^3 - 1.419 \times 10^{-3}\phi^2 + 1.52 \times 10^{-4}\phi + 6.198 \times 10^{-7}$$

and C_{solid} is dependent on the mineral composition. Another relation with porosity can be entered in the tool, but no relation to other parameters. These relations can be made from regression from observations of this parameter (over porosity). A large variation (50-100%) from $C_{frame}(\phi)$ has been observed (e.g. TNO, 2013), caused by differences in e.g. diagenesis, stress history, temperature and pressure (e.g. Arias-Buitrago et al., 2021; MacBeth, 2004). Hence, for a specific porosity, uncertainty in C_{frame} can be evaluated stochastically (see chapter 2.2).

CO_2 density

CO_2 density (ρ_{co_2} in kg/m^3) is a function of pressure in bar and temperature in °C, that is based on thermodynamic properties of carbon dioxide tabulated by Span and Wagner (1996). A surface fit through these tabulated values resulted in a 3rd order polynomial equation:

Equation 11: Relationship between the density of CO_2 and pressure and temperature.

$$\rho_{CO_2} = 260{,}416638 + (-7{,}59534T) + (5{,}587335P) + (0{,}038888T^2) + (-0{,}007272P^2) + (-0{,}000048T^3) + (0{,}000001P^3) + (-0{,}013924TP) + (-0{,}000017T^2P) + (0{,}000026TP^2)$$

The equation's applicability deviates less than 5% from the tabulated values for a pressure range of 150 – 500 bar and a temperature range of 97 – 227 degrees Celsius. Those ranges are assumed common for subsurface aquifer conditions that are considered in this study.

The density of the plume is evaluated for temperatures and pressures at the midpoint of the plume (T_{plume} and P_{plume}). Where P_{plume} is determined by:

Equation 12: Relationship between the maximum plume pressure and depth (assuming gravitational constant $g = 10\frac{m}{s^2}$).

$$P_z^{allowed}(z, \frac{dP_w}{dz}, z_c) = P_{crest}^{allowed} + \frac{\frac{dP_w}{dz}(z - z_c)}{10}$$

evaluated at the midway point between z_c and $z_{injection}$ (z_{plume}).

T_{plume} is based on $\frac{dT}{dz}z$ at z_{plume}.

CO_2 mass calculation

The mass of CO_2 (M_{CO_2}) expressed in kg for aquifer storage is determined by:

Equation 13: Relationship between the CO_2 storage mass and it's four main parameters:

$$M_{CO_2} = V_{pore} C_{total} \Delta P_{crest} \rho_{CO_2}$$

$C_{total}\Delta P_{crest}$ can also be denoted as ε, the efficiency factor, because it relates to the pore space that comes available compared to the entire pore volume (V_{pore}), that is filled with CO_2 at a certain density (ρ_{CO_2}).

2.2 Probabilistic capacity assessment

To take uncertainty of the parameters into account, the storage capacity is also determined stochastically. This is done by drawing the stochastic input parameters from a probability distribution for N (number of samples) amount of times and determining the storage capacity, also called the Monte Carlo method.

For each of the input parameters the probability distribution chosen is the four parameter Beta-distribution $\boldsymbol{B}(x, minimum, mode, maximum, kurtosis)$. Function $\boldsymbol{B}$ is derived from the two-parameter distribution function embedded in Excel ($B(x, \alpha, \beta)$ see Figure 4) adjusting density for specified minimum and maximum values. Using:

Equation 14: Four-parameter beta-function.

$$\boldsymbol{B}(x, minimum, mode, maximum, kurtosis) = minimum + (maximum - minimum)B(x, \alpha, \beta)$$

Where:

$$\alpha = mode^*(kurtosis - 2) + 1$$

$$\beta = kurtosis - \alpha$$

and:

$$mode^* = \frac{mode - minimum}{maximum - minimum}$$

The formulation for $\boldsymbol{B}$ is chosen such, that the minimum and maximum adjust the location on the x-axis and mode and kurtosis adjust the shape of the function. The kurtosis determines how flat or "peaked" the distributions is, where a kurtosis of 1 is a uniform distribution and higher values approach more normally distributed (or "peaked") distributions.

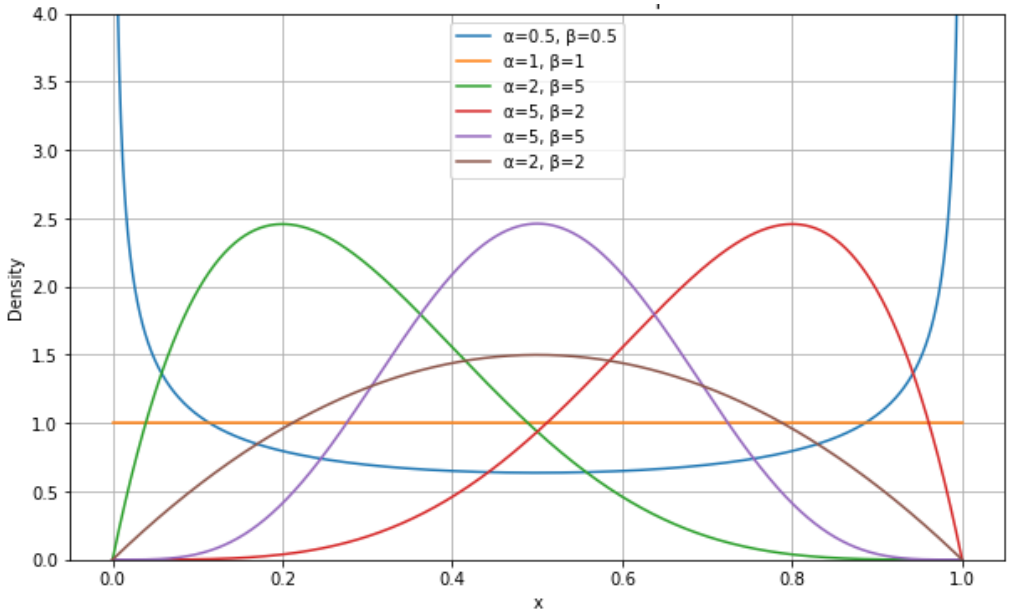

Figure 4: The two-parameter beta function (defined between 0 and 1) with example values for α and β. This figure shows the different shapes of the two-parameter Beta-distribution and it's parameters to approximate common distributions like the uniform (orange), log-normal (green and red) and standard normal (purple) distributions. This figure also includes transitionary distributions (blue and brown).

$\boldsymbol{B}$ is chosen for its finite range and ability to approximate the shape of commonly used distributions. Other distribution (e.g. standard normal or log normal distributions) can have values well outside the range of naturally occurring values because the tail end(s) of the distribution can approach -∞ or ∞ (in rare occasions).

The parameters are considered independent of each other and drawn randomly according to $\boldsymbol{B}$. The exception to how the samples are drawn is C_{frame}, since it is also, but not exclusively, dependent on ϕ. In the stochastic analysis the mode of C_{frame} is determined using $C_{frame}(\phi)$ (see chapter 2.1, Equation 10).

And the minimum and maximum of C_{frame} as:

$$C_{frame}^{min} = C_{frame}^{mode} R_{mode}^{min}$$

$$C_{frame}^{max} = C_{frame}^{mode} R_{mode}^{max}$$

Where R_{mode}^{min} and R_{mode}^{max} are ratios that determine the width of uncertainty. These ratios are assumed or based on experiments. This method captures uncertainty in C_{frame} at a specific ϕ.

Other correlations between parameters exist, e.g. porosity, temperature and salinity are dependent on depth. These correlations are highly dependent on geological context, however, and are filled in as a reservoir average (with relevant uncertainty). The averages are interpreted by a specialist to take these factors into account.

Utrecht, 20th February 2025

W.W. van Driel,

Deputy Research Manager AGE

References

1. Arias-Buitrago, J. A., Alzate-Espinosa, G. A., Arbelaez-Londoño, A., Zambrano-Narvaez, G., & Chalaturnyk, R. (2021). Experimental study on the effect of temperature on the mechanical properties of unconsolidated silty sandstones. Energies, 14(21), 7007.

2. Bentham M., Mallows T., Lowndes J., Green A. 2014, CO2 Storage Evaluation Database (CO2 Stored), the UK's online storage database, Energy Procedia 63, 5103-5113.

3. Gammer D., Green A., Holloway S., Smith G. 2011, The Energy Technologies Institute's UK CO2 Storage Appraisal Project (UKSAP). SPE paper 148426, presented at the SPE Offshore Europe Oil and Gas Conference, Aberdeen.

4. MacBeth, C. (2004). A classification for the pressure-sensitivity properties of a sandstone rock frame. Geophysics, 69(2), 497-510.

5. Span R., Wagner W. 1996, A New Equation of State for Carbon Dioxide Covering the Fluid Region from the Triple-Point Temperature to 1100 K at Pressures up to 800 MPa, Journal of Physical and Chemical Reference Data 25, 1509 (1996).

6. Fjaer et al., 2021, Developments in Petroleum Science, Elsevier, Volume 72.

7. TNO, (2013) Toetsing van de bodemdalingsprognoses en seismische hazard ten gevolge van gaswinning van het Groningen veld. https://www.nlog.nl/sites/default/files/tno_rapport_groningen_15-01-2014_gelakt_pre-scan.pdf

8. Van Buggenum J.M., Davids B., Ravestein T. (2024a) A map-based analysis of the theoretical CO_2 storage capacity in the Rotliegend aquifer of the Dutch offshore. TNO2025 R10216.

9. Van Buggenum J.M., Davids B., Ravestein T. (2024b) SCADSA User guide. TNO2025 R10219.

10. Whitson, C.H., Brulé M., 2000, "Phase Behavior", SPE Monograph Series vol.20, ISBN: 978-1-55563-087-4.

Glossary

- A Area of aquifer in horizontal plane (m^2)
- A_1 A constant in Whitson & Brulé (2000)'s correlation (-)
- A_2 A constant in Whitson & Brulé (2000)'s correlation (-)
- $\boldsymbol{B}$ Beta distribution (-)
- C_{brine} Brine compressibility (1/bar)
- C_{fr} Frame compressibility of formation rock (1/bar)
- C_{fr}^{max} Maximum value for frame compressibility of formation rock (1/bar)
- C_{fr}^{min} Minimum value for frame compressibility of formation rock (1/bar)
- C_{fr}^{mode} Mode value for frame compressibility of formation rock (1/bar)
- C_s Compressibility of grains as solid rock (1/bar)
- C_{total} Total compressibility (1/bar)
- $\frac{dP_w}{dz}$ Hydrostatic gradient (bar/10m)
- $\frac{dT}{dz}$ Temperature gradient (°C/km)
- ϕ Porosity of formation rock (-)
- f_i Interpolation factor (-)
- h_{CO_2} Height of CO_2 plume (m)
- H Thickness of aquifer (m)
- LOT Leak-Off Test
- M_{CO2} Mass of CO_2 injected (kg)
- mid LB-FG Mid Lower Bound-Fracture Gradient (bar/10m)
- N Number of samples (-)
- NtG Net-to-Gross ratio of aquifer (-)
- $P_{crest}^{allowed}$ Allowed pressure at crest (bar)
- $P_{crest}^{initial}$ Initial aquifer pressure at crest (bar)
- ΔP_{crest} Pressure increase at crest (bar)
- P_{crest}^{frac} Fracture pressure at crest (bar)
- $P_{hydrostatic}$ Hydrostatic pressure (bar)
- P_{plume} Pressure at the centre of the CO_2 plume (bar)
- P_z^{frac} Facture pressure profile (bar)
- $P_z^{LOT\ lower\ boundary}$ Pressure based on the lower boundary of Leak-Off Tests (bar)

- ρ_{CO2} Density of CO_2 (kg/m^3)
- R_{mode}^{min} Ratio to determine the minimum relative to a mode (-)
- R_{mode}^{max} Ratio to determine the maximum relative to a mode (-)
- S Salinity of formation water, brine (ppm)
- T Temperature at the center of the aquifer (°F)
- T_{plume} Temperature at the center of the CO_2 plume (°C)
- V_{bulk} Bulk volume of aquifer, which can be inserted or calculated (m^3)
- V_{pore} Pore volume of aquifer (m^3)
- w_s Brine salinity in weight fraction (-), e.g. 0.2 w_s equals 200.000 ppm
- z Depth (mTVDss)
- z_{base} Depth of aquifer base (mTVDss)
- z_{crest} Depth of aquifer crest (mTVDss)
- $z_{injection}$ Depth of injection point (mTVDss)

Energy & Materials Transition

Princetonlaan 6
3584 CB Utrecht
www.tno.nl

TNO innovation for life